Eur. Phys. J. D **55**, 253–264 (2009)
DOI: 10.1140/epjd/e2009-00080-2

THE EUROPEAN PHYSICAL JOURNAL D

Regular Article

Vision of a fully laser-driven nγ−mγ collider

D. Habs[1,2,a], B.M. Hegelich[1,3], J. Schreiber[1], and P.G. Thirolf[1]

[1] Faculty of Physics, Ludwig-Maximilians-University München, 85748 Garching, Germany
[2] Max-Planck Institute of Quantum Optics, 85748 Garching, Germany
[3] Los Alamos National Laboratories, Los Alamos, NM 87545, USA

Received 24 November 2008
Published online 13 March 2009 –

Abstract. The use is suggested of a laser-accelerated dense electron sheet with an energy of ($E = \tilde{\gamma}mc^2$) as a relativistic mirror to reflect coherently a second laser with photon energy $\hbar\omega$, generating by the Doppler boost high-energy γ photons with $\hbar\omega' = 4\tilde{\gamma}^2\hbar\omega$ and short duration [A. Einstein, Annalen der Physik **17**, 891 (1905); D. Habs et al., Appl. Phys. B **93**, 349 (2008)]. Two of these counter-propagating γ beams are focused by the parabolically shaped electron sheets into the interaction region with small, close to diffraction-limited, spot size. Comparing the new $n\gamma$−$m\gamma$ collider with former proposed $\gamma\gamma$ collider schemes we achieve the conversion of many photon-pairs in a small space-time volume to matter-antimatter particles, while in the other discussed setups only two isolated, much more high-energetic photons will be converted, reaching in the new approach much higher energy densities and temperatures. With a γ-field strength somewhat below the Schwinger limit we can reach this complete conversion of the γ bunch energy into e^+e^- or quark-antiquark $q\bar{q}$-plasmas. For a Bose-Einstein condensate (BEC) [A. Einstein, Physikalisch-mathematische Klasse (Berlin) **22**, 261 (1924); A. Einstein, Physikalisch-mathematische Klasse (Berlin) **22**, 3 (1925); A. Griffin, D.W. Snoke, S. Stringari, *Bose-Einstein Condensation* (Cambridge University Press, 1995)] final state or for the Cooper pair ground state at higher densities [A.J. Leggett, *Quantum Liquids*, Oxford Graduate Texts (Oxford University Press, 2006)] the strong induced transition into this coherent state is of special interest for single-cycle γ pulses. Due to annihilation these cold coherent states are very short-lived. For γ beams with photon energies of 1–10 keV the rather cold e^+e^--plasma or e^+e^--BEC expands to a cold dense aggregate of positronium (Ps) atoms, where the production of Ps molecules is discussed. For photon energies of 1–10 MeV we discuss the production of a cold induced π^0-BEC followed by the formation of molecules. For the direct population of higher $q\bar{q}$ densities we can study condensates of color-neutral mesons with enhanced population. For a $\gamma\gamma$ collider with several-cycle laser pulses the following cycles heat up the fermion-antifermion $f\bar{f}$ system to a certain temperature. Thus we can reach high energy densities and temperatures of an $e^+e^-\gamma$ plasma, where the production of hadrons in general or the quark-gluon phase transition can be observed. Within the long-term goal of very high photon energies of about 1 GeV in the $n\gamma$−$m\gamma$-collider, even the electro-weak phase transition or SUSY phase transition could be reached.

PACS. 42.55.Vc X- and gamma-ray lasers – 29.27.-a Beams in particle accelerators – 41.75.Jv Laser-driven acceleration – 41.75.Ht Relativistic electron and positron beams

1 Introduction

We have developed a new concept to produce brilliant γ beams [1], which starts with driving a dense electron sheet out of an ultra-thin, hard, diamond-like-carbon (DLC) foil target by an intense driver laser. This recently has been observed by our group for the first time [2]. The electron sheet is then accelerated within a laser half-cycle to the required energy ($E = \tilde{\gamma}mc^2$) and by injecting a second laser with photon energy $\hbar\omega$ from the appropriate forward direction, it is reflected coherently with high photon energies of $4\tilde{\gamma}^2\hbar\omega$, resulting in brilliant intense γ beams[1]. Here the amplitudes of the scattered photons interfere coherently and add constructively in the direction of reflection. These γ rays can be focused down to small diameters using the properties of the same electron sheet. As neutral beams, very intense small photon bunches can be formed. This new production of brilliant, intense γ beams will be discussed in the first section. It is the fundamental starting element for this contribution.

[a] e-mail: dieter.habs@physik.uni-muenchen.de

[1] We introduce $\tilde{\gamma}$ as a measure for the electron energy to distinguish it from e.g. γ beams.

For 1 eV-photons ($\lambda = 1\ \mu$m) the first order QED two photon scattering cross-section of $\sigma_{\gamma\gamma} \sim 10^{-65}$ cm^2 is that small, that even for 1 J/bunch or about $N_1 = N_2 \sim 10^{19}$ photons in the two bunches focused to a diameter λ the number of reactions:

$$N_R = (N_1 N_2 \sigma_{\gamma\gamma})/(2\pi\sigma_y\sigma_x) \sim 10^{-19} \quad (1)$$

is negligibly small. Here σ_y and σ_x are the vertical and horizontal dimensions of the two photon beams. The QED two-photon scattering cross-section increases with ω^6 (Ref. [3]) and also $\sigma_y \propto \omega^{-1}$ and $\sigma_x \propto \omega^{-1}$. So we have a dependence of $N_R \propto \omega^8$ and we could reach $N_R \gg 1$ for $\hbar\omega \approx 1$ keV and $N_1 \sim 10^{14}$. If we assume $\hbar\omega_1 \sim 1$ keV, a bunch diameter $\lambda_1 = c/\omega_1 \approx 1$ nm and $N_1 = 10^{13}$, we can estimate the energy density ϵ in the interaction volume:

$$\epsilon = (N_1\ 1\ \text{keV}/\lambda_1^3) \sim 1\ \text{MeV}/(386\ \text{fm})^3 \quad (2)$$

where we normalized to the Compton wave length of the electron $\lambda\!\!\!^{-}_e = \hbar/mc = 386$ nm and the rest mass of the e^+e^- pair of 1.02 MeV. For the $n\gamma{-}m\gamma$ collider the dominant process is the *strongly nonlinear interaction* of many photons with virtual fermion-antifermion pairs, leading to the creation of many real fermion-antifermions. The energy density allows to produce many e^+e^- pairs and nonlinear reactions and back reactions are important [4]. While we need a large normalized vector potential a for low energy photon beams (e.g. 5×10^5 for 1 eV) to reach the e^+e^- production, we need a close to 1 for high energy photon beams with e.g. 500 keV. The normalized vector potential is defined by:

$$a = eE\lambda/(2\pi mc^2) = \sqrt{(I_L/1.37 \times 10^{18})[\text{W/cm}^2]\lambda^2[\mu\text{m}^2]} \quad (3)$$

with the field strength E, the wave length λ, and the intensity I_L of the laser. For $a = 1$ an electron gains the energy mc^2 in a half-cycle of the laser and the motion becomes relativistic. On the other hand, if we calculate for $a = 1$ and the Compton wave length of the electron $\lambda\!\!\!^{-}_e$ the field strength E, we obtain the Schwinger field:

$$E_s = m^2c^3/e\hbar = 1.3 \times 10^{18}\ \text{V/m}. \quad (4)$$

While for low photon energies like 1 eV the requirements in focusing are obtained easily, for higher energy photons (e.g. 1 MeV) the requirements on diffraction limited focusing become severe. On the other hand the requirements on the photon number per bunch are very large for low-energy photons, while they become very relaxed for higher photon energies. Even if the pointing stability of the two γ beams would lead only to central hits in a small fraction, the new mode of a collective collider could be used. This total conversion of the bunch energy into the center-of-mass (CM) energy starts at a threshold for the photon energy and for the number of photons per bunch and leads to a new quality of collider physics, with much larger energy and particle densities in the interaction volume. These linear and non-linear QED cross-sections, leading to the production of these dense fermion-antifermion $f\bar{f}$ systems, will be addressed in the second section.

In particle physics the aim to reach high center-of-mass (CM)-energies led to colliders and particle-factories in the 1980's. For charged particles the particles within a bunch repel each other and thus only one particle from a lower density bunch reacts with another one of the counter-propagating bunch. For heavy ion colliders, like the Pb beams of 2.7 TeV/u at LHC, the energy per nucleon is smaller than for the proton beam of 7 TeV, but for heavy ions the total reaction energy and the reaction volume are much larger in central collisions. High energy $\gamma_{high}\gamma_{high}$ colliders with 250 GeV photon beams have been planned, where the photon beams are assumed to be obtained from the NLC electron electron collider, using incoherent laser backscattering from the electron bunches [5,6].

The planned photon number is $N = 10^{10}$, with beam sizes of $\sigma_z = 110\ \mu$m (longitudinally), $\sigma_x = 245$ nm, $\sigma_y = 2.7$ nm (transversely). Thus due to the short wavelength of the photons of $\sim 10^{-2}$ fm again only individual photons of the two bunches react with each other.

In this paper we consider a photon collider with much smaller photon energies in the keV to MeV range, where both bunches in space and time can be close to diffraction limited. While former pp, $p\bar{p}$, e^+e^-, (HI, HI) colliders or the $\gamma_{high}\gamma_{high}$ colliders lead to very hot interaction scenarios, it is conceivable that a bosonic, single cycle standing wave of the new lower energy collider converts cold into a fermion-antifermion ($f\bar{f}$) ground state of a Bose-Einstein condensate (BEC) or pseudo BEC of Cooper pairs. Once the first $f\bar{f}$ pairs are populated, the high critical temperature of the BEC enforces a high population of the ground state and then the transition strength grows exponentially, leading to the predominant BEC population. This will be discussed for a general fermion-antifermion ($f\bar{f}$) system first, but then – in more detail – for the e^+e^- system and the quark-antiquark $q\bar{q}$ system.

If the colliding pulses have several cycles, the cycles after the first one – depending on the field strength – can heat up the BEC to a $f\bar{f}$ plasma, where the temperature can be controlled by the intensity of the following cycles. Via the focusing and the intensity of the two bunches the energy density of the $f\bar{f}$ system is a second free parameter. All systems are charge neutral, color neutral systems. Probably a kind of thermal equilibrium develops between the different $f\bar{f}$ systems like (e^+e^-), ($q\bar{q}$), (SUSY, $\overline{\text{SUSY}}$), which all are rather short-lived for cold systems.

We focus on two types of directly produced systems:

(i) very cold quantum liquids; and

(ii) very hot fermion-antifermion plasmas.

If we produce hot fermion-antifermion ($f\bar{f}$) plasmas they start to equilibrate and expand and one can calculate from the energy density $\epsilon(T)$ the temperature T

$$\epsilon(T) = N_p\, a_B\, T^4/2 \quad (5)$$

where N_p is the number of particle types and a_B is a constant like in the Stefan-Boltzmann law. Phase transitions at critical temperatures T_c change the constants. If we reach rather high thermal energies $k_B * T$, we obtain e.g.

a very broad spectrum of real photon pairs or fermion-antifermion pairs, which can produce new particles. This is similar to the broad virtual $\gamma\gamma$-spectra in peripheral relativistic heavy ion colliders [7]. Though monochromatic excitations of resonances appear more attractive to study specific resonances in this plasma, we can reach much higher photon or fermion-antifermion energies. If at some highest energies new physics with new particles appears, we can select these events by large transverse momenta and study this terra incognita selectively. The thermalization needs some relaxation time, until all degrees are equilibrated. Also this process will be discussed.

The question arises, which are the best photon energies for such a $n\gamma - m\gamma$ collider to reach certain temperatures, densities and particle numbers. For shorter wavelengths the interaction volume decreases with λ^{-3}. On the other hand, the number of produced photons per bunch N_λ will become smaller. The relation $T \propto N_\lambda^{1/4}\,\lambda^{-3/4}$ shows that rather short wavelengths are very interesting. So we plan to proceed gradually to shorter and shorter wave length.

2 The production of brilliant laser-driven γ beams

We pursue the new concept to drive a dense electron sheet out of an ultra-thin diamond-like carbon (DLC) foil [8]. The electron sheet is then accelerated within a half-cycle to its final energy $E = \tilde{\gamma}\, mc^2$ [9]. A second laser with photon energy $\hbar\omega$ is injected opposite to the electron direction and by performing a Lorentz transformation from the laboratory system to the rest frame of the electron sheet and then transforming the reflected pulse back to the laboratory system a Doppler boost with the final energy $\hbar\omega' = 4\tilde{\gamma}^2\,\hbar\omega$ is obtained [10]. The high density of the foil allows for efficient coherent reflection. We furthermore want to increase the reflectivity by trapping the electron sheet between the two lasers, thus preventing the Coulomb expansion. The front laser can be viewed as an optical undulator. The backward accelerating laser acts like a "snowplough" and a density spike is building up, which preferentially reflects the front laser and thus a standing wave develops, which leads to a micro-bunching of the electron sheet. Even if this micro-bunching is incomplete due to the higher electron density, already a fractional micro-bunching is very helpful for the reflectivity. Compared to a classical FEL we require much smaller electron energies for the same γ energy, because the optical undulator has about a 10^4 times smaller wavelength. Furthermore the wavelength in the inner rest frame of the electron sheet is smaller and a micro-bunching has to be achieved over smaller distances. The much smaller electron sheet diameter is advantageous to reduce the requirements on the electron beam parameters. This concept has been described in more detail in reference [1]. Similar to other concepts of reflecting relativistic mirrors [11,12], the mirror can be shaped by the lasers to obtain a focusing, making the approach very efficient. The concept will work best at lower photon energies like 10 keV, where the reflectivity is high, without relying on laser trapping and micro-bunching. Stepwise an extension to higher photon energies in the MeV range is foreseen. Getting close to diffraction-limited γ beams is essential for the proposed $n\gamma - m\gamma$ collider. Here two counter-propagating γ beams are focused in vacuum and an intense fermion-antifermion plasma is generated.

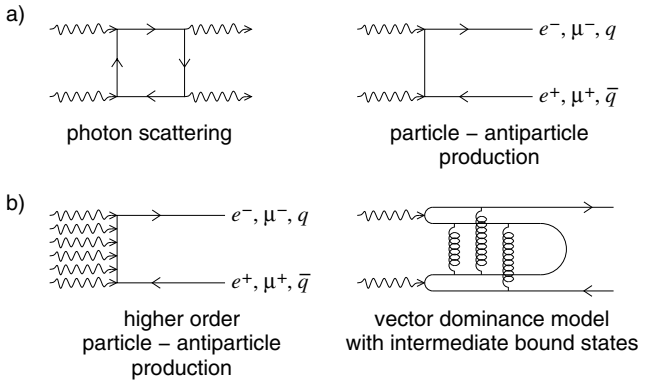

Fig. 1. Feynman diagrams for $\gamma\gamma$ interactions (a) first order processes (b) higher order processes.

On the other hand, with two large, expensive classical XFEL's such a 10 keV collider would be difficult to realize, because they would have to be focused with large losses down to the few nm diameter interaction point. A single cycle pulse contradicts the many periods of the long undulators and both beams would have to be synchronized to the attosecond.

3 The $\gamma\gamma$-cross-section

Next we want to study the $\gamma\gamma$ cross-section to predict the required photon bunch intensities for different photon energies of a $\gamma\gamma$ collider. First we will present the first order linear QED two-photon contributions, but in a second step we discuss the strongly nonlinear multi-photon contributions close to the Schwinger field. One photon has the quantum numbers $J^{PC} = 1^{--}$; thus we produce in two-photon collisions states with $C = +$ and $P = +, J = 0, 2, 3, 4, 5, ...$ and $P = -, J = 0, 2, 4, 6, ...$ For multi-photon reactions we tune for the average spin $\langle J \rangle$ and average $\langle J_z \rangle$ of the fermion-antifermion system, while the parity and charge conjugation can have the values $(--)$ or $(++)$. In a similar way we can tune the average spin and spin projection of the aggregate of fermion-antifermion systems.

3.1 Linear QED contributions of the two-photon cross-section

The lowest order QED cross-sections are obtained from the Feynman diagrams of Figure 1. For low energy photons we have $\gamma\gamma$ scattering. The total $\gamma\gamma \rightarrow \gamma\gamma$ scattering cross section is derived in classical text books [3]. The pure QED

process of $\gamma\gamma$ scattering proportional to α^2 is very small. For $\hbar\omega \ll mc^2$ it shows a ω^6 dependence:

$$\sigma_{\gamma\gamma\to\gamma\gamma} = (973/10125)\,\alpha^2 r_e^2 (\omega/mc^2)^6 \qquad (6)$$

with $r_e = e^2/mc^2 = \alpha\hbar/m_e c = 2.82$ fm being the classical electron radius. It results in an extremely small scattering cross-section for 1 eV photons of about 10^{-65} cm^2 [6], which has not been verified experimentally. On the other hand, for 100 keV γ beams we would have a cross-section of 10^{-35} cm^2, which should lead to reasonable counting rates.

In the high energy limit with $mc^2 \ll \hbar\omega$ we have [3]:

$$\sigma_{\gamma\gamma\to\gamma\gamma} = 4.7\alpha^4\,(c/\omega)^2. \qquad (7)$$

The total photon-photon scattering is given in reference [3] with a kink at $\hbar\omega = mc^2$ and a plateau to 1.5 mc^2. It is shown in Figure 2.

If we would collide 511 keV photons, we should obtain the bound, spin $S = 0$ positronium with a Breit-Wigner resonance. The maximum cross-section $\lambda^2/\pi = 40$ kb is very large, but the lifetime of spin $S = 0$ positronium with $\tau = 125$ ps corresponds to a very small width of $\Gamma = 6$ μeV. Therefore, the resonance is that narrow, that it is experimentally close to impossible to produce γ beams with sufficiently small energy spread and sufficiently high intensity, that matched photon energies $\hbar\omega_1$ and $\hbar\omega_2$ are obtained with $\hbar\omega_1\,\hbar\omega_2 = (m \pm \Gamma)^2\,c^4$ within the width Γ. One can approximate the Breit-Wigner formula for $C = +1$ particles like para-Ps, π^0, η, η_c by a δ function [13] with a resonance mass m and obtains:

$$\sigma_{\gamma\gamma} = (8\pi^2/m\tau))\delta(m^2 - 4\omega_1\omega_2). \qquad (8)$$

For e^+e^- pairs the reaction occurs in a very small volume of the Compton wavelength of the electron of $\lambda\!\!\!^{-} = 386$ fm, while the produced Ps is many orders of magnitude larger with 2 Å. Thus a tunneling out to this much larger configuration occurs from the production centre.

Above the resonance the integral cross-section for charged fermion pair production in two-photon collisions to lowest order in QED [7] is:

$$\sigma(\gamma\gamma \to f^+f^-) = [(4\pi Q_f^4\,N_c\,\beta)/s]\,A \qquad (9)$$

$$A = [((3-\beta^4)/2\beta)\ln(1+\beta)/(1-\beta) - 2 + \beta^2] \qquad (10)$$

where $s = (p_1 + p_2)^2 = 4E^2$ is the square of the center of mass energy. Q_f is the fermion charge in units of e, N_c the number of color degrees of freedom, and $\beta = \sqrt{1 - 4m_f^2/s}$ is the velocity in the $\gamma\gamma$ rest frame. The maximum cross-section for $\gamma\gamma \to e^+e^-$ pairs is 17 fm^2 = 170 mb. The $1/s$ dependence leads to the high-energy fall off. If the γ beams are focused sufficiently (small σ_x, σ_y) and have sufficient photon numbers N_1, N_2 per bunch, one converts all photons into a high energy density of an $e^+e^-\gamma$-plasma, where secondary $\gamma\gamma$ and e^+e^- reactions can create more heavy constituents. In Figure 2 the production cross-section of these e^+e^- pairs is shown, followed at higher energies by the π^0 resonance. Above the two pion threshold the quark-antiquark $q\bar{q}$ production sets in. Then overlapping resonances with two-photon quantum numbers contribute, where the nonlinear cross-sections of the vector dominance model (VDM) have to be used. Between 1–100 GeV we show in Figure 2 the measured hadron production from $\gamma\gamma$ reactions [14].

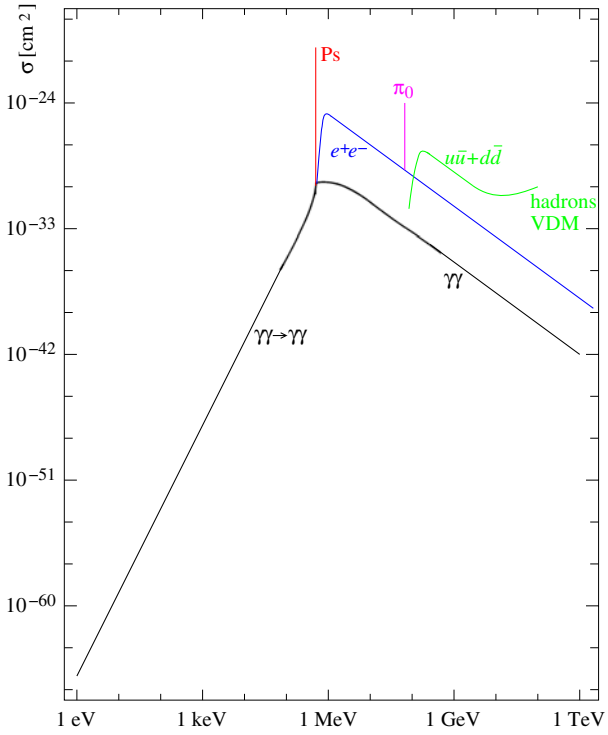

Fig. 2. (Color online) $\gamma\gamma$ cross-section from perturbative QED. We show the hadronic cross-section in green, the e^+e^- cross-section in red and the $\gamma\gamma$ scattering in black.

3.2 Nonlinear QED contributions in $n\gamma + m\gamma \to e^+e^-$ production

For the production of e^+e^- pairs in intense $n\gamma - m\gamma$ collisions nonlinear processes have to be studied. Let us assume that we collide two diffraction limited, linearly polarized beams with diameter λ and pulse duration λ/c in such a way, that in the centre the B fields cancel and the E fields add up to $E_s \sin\tau$. In a first rough approximation we assume that each beam has the field strength $E_s/2$ with E_s being the Schwinger field. The beams have the intensity:

$$I_s = (c\epsilon_0/4\pi)\,(E_s/2)^2 = 1.2 \times 10^{29}\ \mathrm{W/cm^2}. \qquad (11)$$

We make the rough assumption – which is justified later – that in this case one e^+e^- pair is produced per collision. Then we obtain the necessary photon number:

$$N_{min}(\hbar\omega) = I_s\,(2\pi)^3 c^2/(\hbar\omega^4) = (1/4)\,[511\ \mathrm{keV}/(\hbar\,\omega)]^4. \qquad (12)$$

For 511 keV photons we obtain $N_{min}(511\text{ keV}) = 1/4$; for 10 keV photons $N_{min}(10\text{ keV}) = 10^6$ and for 1 eV photons $N_{min} = 10^{22}$. The numbers approximately agree for the 1 eV and 10 keV photons with the numbers of reference [15,16]. The interaction volume $(2\pi c/\omega)^3$ is much larger than the volume with the electron Compton wavelength λ_e^3 and we mostly have multi-photon tunneling processes and the estimate that we approximately produce just one e^+e^- pair is derived in references [15,16]. In a detailed investigation of two colliding photon beams with 1 eV the threshold intensity for one e^+e^- pair was determined to be under optimum conditions $I_{sc} = 10^{26}$ W/cm^2 [4]. Rescaling the photon number leads to:

$$N_{sc}(\hbar\omega) = I_s\,(2\pi)^3\,c^2/(\hbar\omega^4) = [511\text{ keV}/(2.7\,\hbar\omega]^4 \quad (13)$$

here we obtain $N_{sc}(511\text{ keV}) = 1/50$; $N_{sc}(10\text{ keV}) = 1.3\times 10^5$ and $N_{sc}(1\text{ eV}) = 1.2\times 10^{21}$.

From equation (7) we obtained a maximum cross-section of $\sigma_{\gamma\gamma\to e^+e^-} \approx 170$ mb and for one e^+e^- event with diffraction limited beams 10^3 photons/bunch, which for this linear first order cross-section is correspondingly larger than the value of $N_{sc}(550\text{ keV}) = 2\times 10^{-2}$.

Since it will be difficult to reach the very small bunch diameter of 2 pm for 511 keV photons and at the same time it will be difficult to reach the photon number per bunch of 10^{22}, corresponding to 1.5 EW for 1 eV photons, it seems best to start with a beam of 10 keV and 10 TW and a beam diameter of 0.1 nm. Once the particle number N surpasses N_{sc}, the conversion to e^+e^- pair increases exponentially and soon all energy of both beams is converted fully into an $e^+e^-\gamma$-plasma and one obtains a maximum energy density:

$$\epsilon(\hbar\omega) = 2\,(2\pi)^3\,(N/N_{sc})\,\hbar\omega^4/c^3 \quad (14)$$

$$\epsilon(\hbar\omega) \approx (N/N_{sc})\,(\hbar\omega/mc^2)^4\,100[\text{MeV/pm}^3]. \quad (15)$$

In our new production scheme of X rays we have to optimize the reflectivity of the electron sheet, the shape of the electron sheet for focusing and the intensity of the reflected laser. Since N_{sc} will be significantly smaller than the obtained photon numbers, we can relax the condition of diffraction limited focusing.

Gradually one will increase the photon energy to reach higher energy densities. If we focus the two photon beams less, still with 10^{12} photons/bunch a complete conversion is reached and the primary produced e^+e^- pairs will be much more separated before they tunnel to Ps atoms.

For higher γ energies like 1 MeV, we have the sequence $n\gamma$–$m\gamma \to e^+e^-\gamma \to \gamma_{high}\gamma_{high} \to \pi^0$ (for counterpropagating γ_{high}) and $\pi^0\pi^0 \to \pi^+\pi^-$ reaching a hadron plasma or $n\gamma$–$m\gamma \to \pi^0$BEC. For still larger energy densities we reach the quark-gluon plasma. So one has to compare the production efficiency and focusability of hard γ rays with the loss in temperature by expansion of the $e^+e^-\gamma$-plasma. At present it seems best to reach for 1 MeV photons and to produce larger temperatures via the $e^+e^-\gamma$-plasma.

4 Quantum liquids with Bose-Einstein condensation and Cooper pairing

Usually one expects to produce in head-on collisions of a collider a very hot plasma. Here the transition of the bosonic condensed photons with rest mass zero, forming a standing wave, into another bosonic cold configuration, dominated by quantum mechanics, may be unique. We want to study the question at which temperatures quantum liquids, showing quantum mechanical effects, can be produced. Some of the basic ideas are:

- the quantum liquids have one favored condensed bosonic state – the ground state – which can acquire a strongly enhanced production probability, proportional to the number of particles in the state, favoring the production at temperature $T = 0$;
- the requirement for Cooper pairs with opposite momenta is automatically fulfilled for locally produced fermion-antifermion pairs;
- the very strong energy dependence of multi-photon tunneling favoring the production of very cold systems;
- once all energy is transferred in a cold conversion, no electrical fields remain to heat up the new condensate;
- the laser pulses of the two bunches should be as short as possible, so that the produced quantum liquid is not heated up after production. Thus strong single-cycle pulses with a cosine-shaped envelope are necessary.

For quantum liquids quantum mechanical effects become important, when the interparticle distance $d = n^{1/3}$ (n = particle + anti-particle density) compared to the de Broglie wavelength $\lambda = h/p$ fulfills the relation $d \le \lambda$. With the momentum $p \approx (mk_BT)^{1/2}$ we obtain the relation:

$$k_BT \le n^{2/3}\hbar^2/m \quad (16)$$

where m is the mass of the produced fermions or antifermions. Here very light particles like electrons or light quarks are favorable for high temperatures T. For the same reason we are interested in rather high particle densities.

For colliding photons the chemical potential $\mu = 0$ as considered originally by Bose [17]. However, let us first assume that we produce $f\bar{f}$ systems – like positronium (e^+e^-) – as bound bosons and as a dilute, non-interacting gas, and that the $f\bar{f} \to \gamma\gamma$ annihilation is rather long-lived compared to the rather short time interval considered and that we have a constant effective number N_b of bosons with mass m. In this case the relativistic chemical potential μ is non-zero. Frequently also the canonical conjugate density n is displayed in plots. With the thermal wave length $\lambda_{th} = \hbar\sqrt{2\pi/mT}$:

$$n = (g/\lambda_{th}^3)\,\exp(\mu - m - U/kT) \quad (17)$$

with the nonrelativistic potential u and the degeneracy factor g. For noninteracting bosons Einstein's theory [18] predicts a Bose-Einstein condensate. For more realistic situations the interaction between $f\bar{f}$ bosons – e.g. the dipole-dipole interaction between Ps atoms – has to be

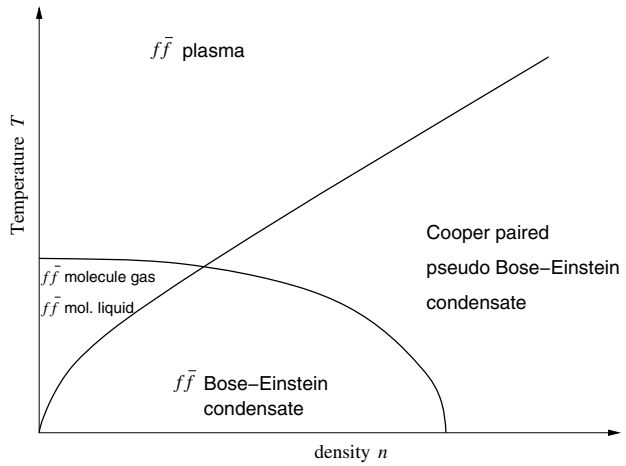

Fig. 3. Generic phase diagram for a fermion-antifermion ($f\bar{f}$) system. For very low temperatures and densities a Bose-Einstein condensate of $f\bar{f}$ molecules is formed. For high densities long range correlated Cooper pairs are formed, which condensate into a pseudo Bose-Einstein condensate. For high temperatures a plasma of f and $\bar{f}$ particles exists.

considered. For Ps and π_0 condensates have been discussed [19,20].

Since Bose-Einstein condensates are more easily to understand and since pseudo BEC's may also be reached via Cooper pairing, we discuss both theories on equal footing. The generic phase diagram for the fermion-antifermion ($f\bar{f}$) system is shown in Figure 3 as a function of temperature T and density n. A curve $T \propto n^{2/3}$ separates the quantum mechanical condensates from the particles behaving like classical particles. A second curve marks the phase transition between the $f\bar{f}$ plasma and the bound $f\bar{f}$ systems. For high densities n and lower temperatures this phase transition is continued between the BEC condensate, bound $f\bar{f}$ systems and the pseudo BEC's of Cooper pairs, where the high density prevents forming local bosonic $f\bar{f}$ systems.

The produced fermion-antifermion pairs can form bound bosonic systems, like in positronium for e^+e^- pairs or in mesons for $q\bar{q}$ pairs. These bound systems, which due to the steep exponential energy dependence of the reaction are produced at low temperatures, may condense into the ground state of a Bose-Einstein condensate (BEC) [18,21,22]. Since the transition matrix element grows with the number N_{BEC} of particles in the BEC, we have an exponential growth into this ground state. Once we overcome the threshold, all photon energy is transfered into this BEC. Since the BEC is not in a trap – due to the confined production and momenta within the uncertainty principle – it will expand. For a given density n we can calculate the critical temperature T_c for a free Bose-Einstein condensate [21] and with the given temperature T we obtain the fraction f of being in the BEC ground state:

$$T_c = 1/2\,(\pi\hbar^2 n^{2/3})/mk_B \tag{18}$$

$$f = 1 - (T/T_c)^{3/2}. \tag{19}$$

It is interesting to note that T_c is of the same order as the Fermi temperature T_F for a Fermi system with the same mass m and density n. The Fermi temperature is given by:

$$T_F = p_F^2/(2\ k_B\ m) \tag{20}$$

the Fermi momentum by:

$$p_F = ((3n\,(2\pi\hbar)^3)/(4\pi))^{1/3}. \tag{21}$$

When reducing the density n the critical temperature T_c is lowered and the fraction f is reduced. For temperatures close to T_c large fluctuations occur and cold molecules like Ps_2 or $(\pi^+\pi^-)_n$ can be formed. So the cold BEC can be an interesting intermediate step to cold molecular systems.

Besides the tightly bound bosonic fermion-antifermion systems, which form BEC's for low densities n, it is possible to form much more extended scattering states with an interaction, which also condense into a coherent superfluid state. These BCS states occur in the high-density limit and this process of the formation of Cooper pairs and their condensation are essentially identical [22]. Since the critical temperature scales with $n^{2/3}$, here much higher temperatures of e.g. 1 MeV for e^+e^- pairs or 100 MeV for color superconductors could be reached. While BEC systems have been discussed for e^+e^- [19], Cooper pairs have not been considered until now. Here we treat for e^+e^- neutral pairs of superfluidity, while the electron Cooper pairs of the BCS theory correspond to superconductivity. Though the attraction between e^+e^- pairs is reduced by Debye screening, only an infinitely small remaining interaction is sufficient to form Cooper pairs. For quarks and antiquarks one correspondingly should discuss color superfluidity, which has not been investigated until now. Here only the color superconducting Cooper pairs of the qq systems and not $q\bar{q}$ systems have been discussed. Our systems have a chemical potential $\mu \neq 0$. On the other hand we introduce independently from T the density n of fermion-antifermion pairs as independent parameter. Since all our systems can decay by two photons, we study very short-lived systems, which have not been investigated so far, however, compared to the as-zs γ pulses of the collider they are long-lived.

If the system with the BEC acquires some temperature T, there is a very different behaviour for e^+e^- pairs and $q\bar{q}$ pairs. The low binding energy $E_B = 6.8$ eV of Ps leads to a breakup of the bosonic pair for temperatures with $T > E_B$. Also if the density is larger than closely-packed Ps atoms, the fermionic substructure will overwhelm the bosonic structure.

For mesons, due to the phase transition from the quark-gluon-plasma at $T_{QGP} = 170$ MeV, the BEC realization is not hampered by the breakup into fermions. For the pion condensate, on the other hand, one has to realize that the mass used to calculate the Schwinger field is a factor of 140 larger. Therefore it will require $\sim 10^4$ times higher intensities in the γ beams to reach the threshold for direct pion production, but then the strong enhancement due to populating the BEC state will lead to this exponentially enhanced production of the BEC ground state.

4.1 Hot ultra-relativistic fermion-antifermion plasmas

The opposite extreme to cold quantum liquids are ultra-relativistic fermion-antifermion plasmas. While for cold systems the fast annihilation limits the investigations – although we work with as or zs pulses – for hot plasmas the overlap between particles and antiparticles is strongly reduced and annihilation becomes irrelevant. Thus also in astrophysics these systems are important. In Pb+Pb collisions with 2.7 TeV/u at CERN the QGP is produced in the same way. We can produce the same energy density by colliding two γ beams with the photon energy $\hbar\omega$ as an additional free parameter. When we produce particles with an energy E_T, the multiphoton parameter $K = E_T/\hbar\omega$ determines the power of the increase of the nonlinear tunneling process [23]. High powers will lead to smaller temperatures for the same energy density. In this way we can vary the temperature T independently of the energy density ϵ and populate different points in the (T, ϵ) phase diagram. Similar to the plasmas produced in heavy ion collisions, afterwards an expansion and equilibration occurs. Here we can diagnose the spatial and time-like development in the as-zs time range by diffraction studies, while presently in high-energy physics only the hadronization of the decay products is measured. Presently only the quasi-thermal equilibrium is studied, but we will be able to investigate the relaxation processes towards this equilibrium.

5 Special fermion-antifermion ($f\bar{f}$) systems

In the following we want to discuss the e^+e^- system and the $q\bar{q}$ system in more detail. The e^+e^- system is more important in the near future, because it can be reached more easily.

5.1 The e^+e^--phases

In Figure 4 we show the phase diagram of QED for the e^+e^- systems similar to the general $f\bar{f}$ system of Figure 3.

The bound system of an electron and a positron, the positronium (Ps), was discovered by Deutsch in 1951 [24,25] with a binding energy $E_B = 6.8$ eV and a diameter of 2 Å. The ground state is the $S = 0$ para-positronium, which decays into two diametral 511 keV photons with a halflife of 125 ps. Only ∼1 meV above this $S = 0$ ground state is the isomeric $S = 1$ ortho-positronium ground state, which decays into three γ rays with a halflife of 143 ns.

In 1946 Wheeler [26] suggested that clusters of electrons and positrons may form bound systems, which he called "polyelectrons". He wanted to explain in this way mesons, which were newly discovered at that time. In 1981 the positronium ion Ps^-, consisting of a positronium and an attached electron was identified by Mills [27]. It has a binding energy of ∼0.33 eV, no excited state, a halflife of 0.5 ns and a triangular shape.

Two positronium atoms form a di-positronium molecule Ps_2 with the shape of a triangular pyramid and

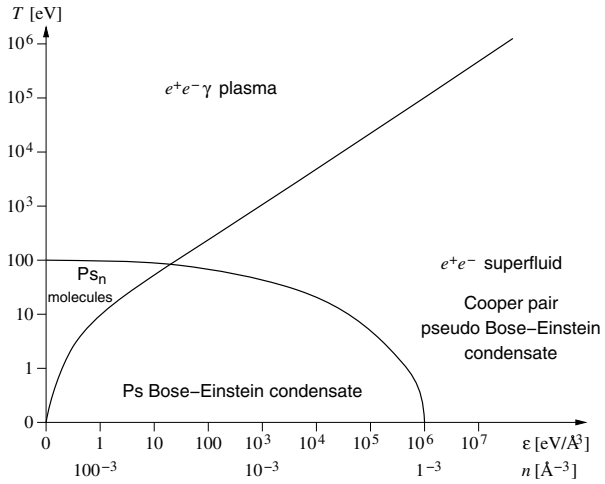

Fig. 4. QED-phase diagram with electrons, positrons and γ quanta. The e^+e^- pairs may form a bound positronium atom Ps at lower temperatures and densities. n Ps atoms may combine to a Ps_n molecule. At very low temperatures a Bose-Einstein condensate of Ps is predicted [29]. For high densities a Cooper pair condensate may form.

a binding energy of 0.435 eV. The spins of the electrons and positrons are opposite ($S_e = 0, S_p = 0$) for Ps_2 in the ground state and the total spin $S = 0$ and $C = +$ and $P = +$. Here the matter-antimatter symmetries lead to new quantum numbers. Ps_2 has a second bound state with orbital angular momentum $L = 1$, negative parity and $S = 0$ with a binding energy of 0.596 eV [28]. Finally, in 2007 the production of this di-positronium molecule Ps_2 was reported [29]. Ps_2 molecules are the "ultimate nonrigid" molecules [30]. Since there are no heavy slowly moving nuclei, like in ordinary molecules, all is smeared out and exchanged in relativistic motion of the leptons, so that geometrical pictures have large width $(\Delta R)^2$ in the spatial separations between leptons. Still it may be useful to describe Ps_2 by a triangular pyramid [31].

In Figure 5 we show the structures of Ps, the Ps^- ion and Ps molecules. Presently the ground states of larger aggregates of positronium Ps_n with $n > 2$ are studied theoretically [30] for different spins. The aggregates can be characterized by conserved quantities, like the total spin S, the projection of the total spin S_z, the charge conjugation parity C and the inversion parity P. Until now it was not possible to study positronium systems with more than one e^+ in detail, because the necessary high densities of anti-matter could not be reached.

Since we think that we now can realize much higher densities of e^+e^- systems, we can discuss BEC's of these systems, which may lead to cold Ps molecules. The BEC's are of special interest, because we can obtain a strongly enhanced stimulated production of these bosonic final states. For Ps the formula for the critical temperature T_c for a Bose-Einstein condensate gives:

$$T_c = 1/2\,(\pi\hbar^2 n^{2/3})/m_e k_B = 734\,T[K]\,(n \times 10^{-21}\ \mathrm{cm}^3)^{2/3}. \quad (22)$$

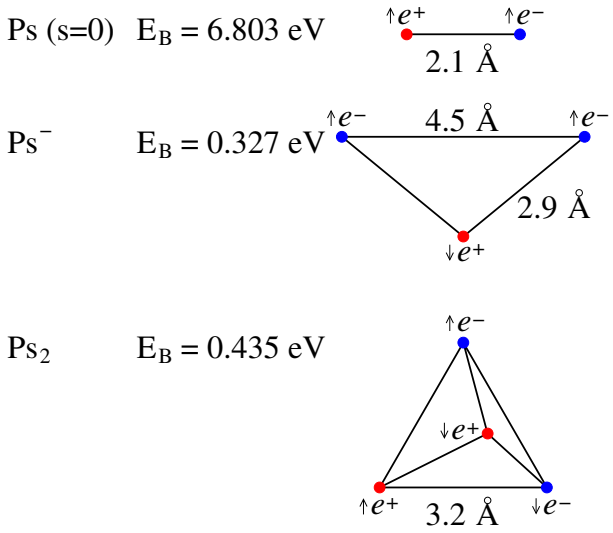

Fig. 5. (Color online) Multi-positronium configurations.

The temperature is very large compared to other BEC's, because the mass of Ps is very small and its Compton wave length is very large [32]. Thus we reach a BEC near room temperature due to the small mass of Ps and the attainable densities. The Bose-Einstein condensate will have a complex phase diagram due to the 4 spins states. The $m = 0$ Ps may separate into phases of binding and unbinding states. Since we have a free control on the spin distribution, we can disentangle this complex phase diagram. The critical density of positronium is $\sim 10^{23}/\mathrm{cm}^3$ with a critical temperature of $\sim T_c = 0.1$ eV.

Besides the tightly bound Ps atoms one could also form a condensate of spatially much larger scattering systems, where the e^+e^- pairs interact via the long-range Coulomb attraction and form a superfluid coherent state. For high densities we show in Figure 4 this region of Cooper pairs forming a pseudo Bose-Einstein condensate, described by the BCS theory. The gap Δ is approximately equal to the Fermi energy of the equivalent Fermi system. Since the Fermi energy increases with $n^{3/2}$, much higher temperatures can be reached for the condensate. After production this BCS condensate may cool by γ emission and expand. Thus finally rather cold expanded systems may be reached, which may decay into Ps molecules.

In Figure 4 we showed the phase transition line, where the gas of Ps atoms transforms into an e^+e^- plasma, because either the temperature becomes too high compared to the binding energy, or the density exceeds the density of closely-packed Ps atoms. This phase diagram of QED is similar to the phase diagram of QCD with quarks, antiquarks and gluons (see Fig. 6), but the different color and flavor degrees of freedom of the quarks lead to a much richer phase diagram.

In future experiments we want to address first *cold multi-positronium*, where we want to produce a very cold e^+e^- plasma with lower density. It is probably the best to produce it via a Ps Bose-Einstein condensate (BEC). We want to use 10 keV γ beams focused to an optimum interaction volume and an energy spread of both γ beams of 10^{-3}, so that the fraction $f = 1 - (T/T_c)^2$ in the condensate would be 3/4 for $T = T_c/2$. Thus most of the positrons would be produced in the BEC. The coherent BEC ground state should enhance the transition rate into this very cold configuration. The expanding BEC at the critical temperature will have large fluctuations favoring the production of Ps molecules and ions. Here three-body interactions have to stabilize the Ps-molecule formation. In this way also large molecules of Ps_n could be produced. These unique purely leptonic, mesoscopic matter-antimatter systems can be studied for the first time due to the high e^+e^- space density. It has many aggregates and phases, which are of scientific interest. We could study collective modes and study the structure by diffraction analysis. Also applications like an intense annihilation laser [29] with very energy sharp 511 keV entangled photons can be explored.

A detailed PET-like diagnostics will allow to optimize the collider (spotsize, overlap of the γ beams) and study the aggregates. We can perform a diffraction analysis of these short-lived systems with a well timed further X-ray laser.

For two colliding beams with opposite spin we produce via multi-photon conversion $S = 0$ singulet positronium, called para-positronium (p-Ps), and $S = 1$ triplet positronium, called ortho-positronium (o-Ps), because an uneven number of photons merge for $S = 1$. We can tune the elliptically polarized γ beams such that we get on the average a certain spin expectation value $\langle S \rangle$ and a certain projection $\langle S_z \rangle$. Thus we can select the average spins of the pairs and of the whole ensemble. The production mechanism requires to produce many e^+e^- pairs with a typical density of $1/\mathrm{Å}^3$, corresponding via the uncertainty principle to a kinetic energy of ~100 eV, which is in the range of the binding energy of –6.8 eV for Ps.

5.2 The qq̄ gluon phases

Figure 6 shows the well known phase diagram for the quark-quark gluon systems described in the framework of QCD with the temperature T as a function of the chemical potential μ [33]. Depending on the temperature T and μ, this strongly interacting matter occurs in three distinct phases: the hadronic phase, the quark gluon plasma (QGP) and the color superconducting quark matter. Above 170 MeV for small densities also a QCD liquid and for somewhat higher temperatures a QCD gas is discussed. The ground state of infinite nuclear matter occurs for $T = 0$, a density of $0.14/\mathrm{fm}^3$ or a chemical potential $\mu = 300$ MeV. There is a line of a first-order phase transition for the liquid-to-gaseous nuclear phase transition ending at a critical end point with $T_c \sim 19$ MeV. Beyond the critical endpoint there is no distinction between the two phases. In a similar way we have a curve for a phase transition of the strongly interacting hadronic matter. This line marks the first-order phase transition

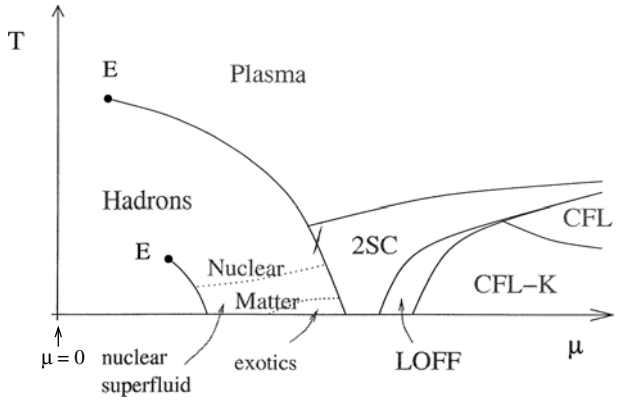

Fig. 6. QCD phase diagram with the temperature T as a function of the chemical potential μ. For high densities the attractive fermion-fermion interaction is predicted to lead to different pair condensates of color superconductivity [33]. CFL = **C**olor-**F**lavor-**L**ocking; CFL-K = CFL with **K**aon condensate; 2SC = 2 flavor color **S**uper-**C**onductor; LOFF = Larkin-Ovchinikov-Fulde-Ferell.

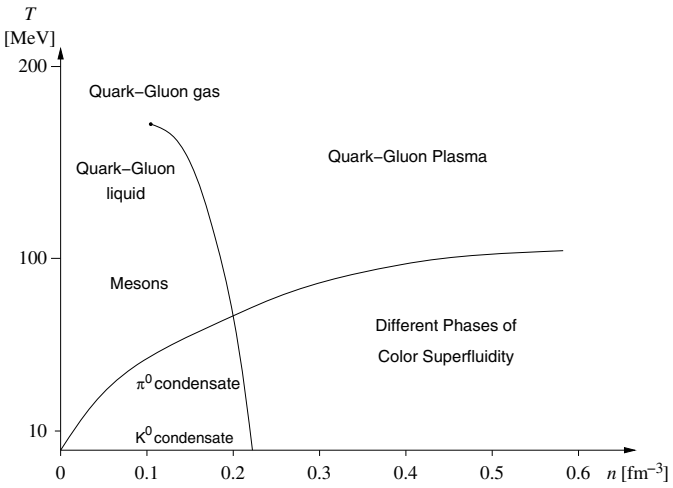

Fig. 7. QCD phase diagram for color and charge neutral systems where the temperature T is shown as a function of the density of fermion- and antifermion pairs. Though we do not know theoretical predictions for this phase diagram, we assume that the condensates between fermions and antifermions form similar condensates like in the diagram with the chemical potential and that on top then correlations occur between these colored condensates, finally leading to the color and charge neutral condensates.

between the hadronic phase and the QGP. It terminates also at a critical point, where the transition becomes second order with $T_c \sim 170$ MeV and $\mu_c \sim 240$ MeV. At large quark chemical potentials or densities and smaller temperatures we have the deconfined color superconducting phase, where quark pairs feel an attractive gluon interaction and a multitude of different bosonic phases are predicted [33,34]. Since the interaction is mediated by color forces in QCD and the quarks form Cooper pairs similar to the electrons in a metallic superconductor, the states are called color superconductors. The pairing gaps can be of the order of 100 MeV.

With our $n\gamma$–$m\gamma$ collider we, however, produce only systems with no charge and color. We can introduce a new orthogonal axis to the temperature T with the density of produced fermion anti-fermion pairs and plot a new phase diagram shown in Figure 7. We plot the situation of quark-antiquark pairs in a similar way, though it is an unproven extrapolation that these condensates look similar. We added the curve for the critical temperatures T_c of the pion and K^0 condensates. We assume that the quarks and the antiquark systems form color superconductors like in the conventional phase diagram, but then a united color neutral system with additional correlations between fermion and anti-fermions is formed. Though it is color neutral, similar superfluid phases may exist. All these bosonic BEC phases are of special interest to us due to the enhanced production cross-section. Thus we aim at studying these phases for the first time. When it becomes possible to obtain the much higher photon energies with diffraction limited focusing, then this leads to much higher energies and avoids the expanding process of producing the higher photon energies in the $e^+e^-\gamma$ plasma.

There are several diagnostic tools at hand to study these new phases: like in present high energy physics we can study the decay products after hadronization, where hopefully detailed theoretical predictions can be obtained. We can use γ ray diffraction analysis to measure with a third γ ray laser the charge density distribution on the zs-as time scale after producing the $q\bar{q}$ system in the $n\gamma$–$m\gamma$ collider. Compared to the present production of the QGP in heavy ion collisions, we have much better defined starting conditions and can use the ultra-fast "pump-probe" techniques to follow the space-time evolution. Furthermore we can study the produced systems as a function of the total spin as an important additional degree of freedom.

5.2.1 Cold pion and kaon condensates

If we tune the collider to densities above the nuclear density and temperatures below 100 MeV, we first will produce a condensate of π^0 and for higher densities a condensate of K^0. The pions have a mass of 140 MeV and decays with a lifetime of 84 as into two γ rays at 68.9 MeV. Although this rather short lifetime, we can work with much shorter γ-ray pulses and probe the structure of the pion condensate. While the pion has the structure $\pi_0 = (u\,\bar{u} - d\,\bar{d})/\sqrt{2}$, the K^0 has the structure $d\bar{s}$ and the $\bar{K}^0$ the structure $\bar{d}s$. There exist the two mixtures $K_S = \sqrt{1/2}(K^0 + \bar{K}^0)$ with CP = +1 and $K_L = \sqrt{1/2}(K^0 - \bar{K}^0)$ with CP = –1. K_S (short) has a lifetime of 0.089 ns and K_L (long) a lifetime of 51.7 ns.

We expect that the π^0 BEC is not an ideal condensate without interaction, but that σ mesons are exchanged between two π^0 in the s state, corresponding to an attractive interaction. For p states a ρ meson is exchanged. However, for BEC's one wants to have a weak repulsive interaction, while for an attractive interaction a fragmentation into several components is predicted. These condensates are quite different from the condensate of pions and kaons in nuclei, where the interaction with the nucleons leads to a lowering of the boson masses and a type of restauration of the Goldstone bosons with chiral symmetry [35].

Once the free π^0 condensate wave function expands, which due to the confined production via the uncertainty relation has a broad spectrum of momentum components, the critical temperature is reduced and more and more π^0's leave the BEC state and strong fluctuations occur. Then, via the reaction $\pi^0 + \pi^0 \rightarrow \pi^+\pi^-$, $\pi^+\pi^-$ pairs can be formed, which are much more long-lived and can form bound systems similar to Ps. Even molecules similar to Ps_2 like $(\pi^+\pi^-)_2$ can be formed. The atoms $\pi^+\pi^-$ may even survive the decay into $\mu^+\mu^-$, if the neutrinos are Majorana particles and induced transitions of the second pion occur.

6 Hot fermion-antifermion plasmas

6.1 $e^+e^-\gamma$ plasma at about T = 10 MeV

We can produce in the $n\gamma$–$m\gamma$ collider a hot $e^+e^-\gamma$ plasma, which will thermalize according to its energy density. It is an interesting plasma on its own and has been studied in reference [36]. Via photon pairs or e^+e^- pairs pions may be produced, a process studied in reference [37]. In both references the hot $e^+e^-\gamma$ plasma was assumed to be produced by two circular polarized laser beams, which compress and accelerate electrons in a gold foil that much, that the electrons produce positrons in the field of the high Z nucleus [38]. Here, however, we produce the hot $e^+e^-\gamma$ plasma with the $n\gamma$–$m\gamma$ collider.

With 1–10 MeV γ beams we can produce cold quarkonium systems similar to the positronium system for the high energy density in the small interaction volume. Again studying in a similar way for the up and down quarks the π^0 BEC, $\pi^+\pi^-$ atoms or $\pi^+\pi^-$ molecules, or for the $s\bar{s}$ system, the η meson at 549 MeV, or for $c\bar{c}$ the η_c at 2981 MeV. Replacing the 1 MeV mass of the Ps by the 140 MeV of the π^0 reduces the critical temperature via the Compton wavelength. On the other hand we now focus not 10 keV photons but 10 MeV photons with a 10^3-fold reduction in wavelength, thus increasing the density by up to 10^9 and the critical temperature by 10^6. The hot $e^+e^-\gamma$ plasma is of interest by itself [36] and the production of hadrons by the interaction of photon pairs or electron positron pairs can be studied [37]. Here new collective modes of ultrarelativistic e^+e^- plasmas like the fermionic plasmino mode have been predicted [36]. In diagnostics the two diametrally 69.8 MeV photons from the π^0 decay can be used in a similar way like the 511 keV photons from the $S = 0$ positronium. Also the delayed muon decay will provide a good diagnostics.

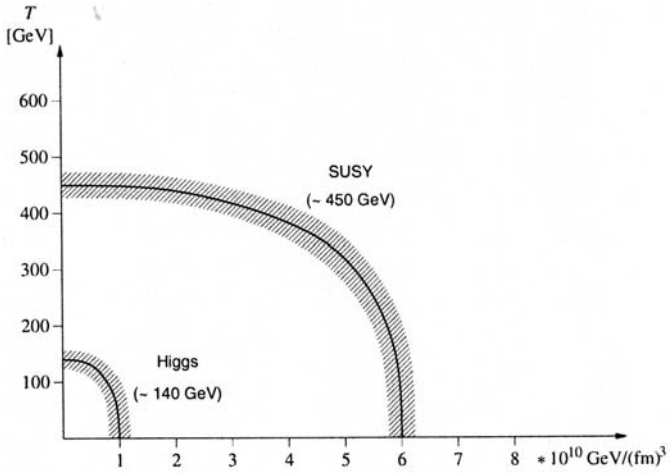

Fig. 8. Diagram of the electroweak and SUSY phase transition.

6.2 $e^+e^-\gamma$ plasma above T = 170 MeV

When colliding high energy photons of e.g. 100 MeV [1] we can produce an $e^+e^-\gamma$-plasma above $T = 170$ MeV and $\mu = 200$ MeV, which forms a quark-gluon plasma (QGP) and will hadronize after a short time. We can use all the high energy physics methods developed at RHIC to prove the production of this QGP, like quenched jets or J/Ψ suppression [39]. Here it may be interesting to probe the critical point.

7 New phase transitions at the highest energies

Figure 8 shows a schematic phase diagram of the electroweak and the supersymmetric (SUSY) phase transitions. In a spontaneous symmetry breaking, the scalar Higgs boson (∼(120–160) GeV) gives masses to the W^{+-} vector bosons at 80 GeV and and the Z^0 vector boson at 91 GeV. This breaking of the electroweak gauge symmetry corresponds to a phase transition. The vector bosons of the weak interaction are equivalent to the gluons of QCD, where the chiral symmetry breaking corresponds to the phase transition between hadrons and the quark gluon phase. In a similar way the supersymmetric theories show a strong symmetry breaking expressed by the lightest SUSY particle, the neutralino, as a candidate for dark matter. Astronomical measurements have been reported, where an annihilation $\chi + \bar{\chi} \leftrightarrow f + \bar{f}$ or dark matter particle $\leftrightarrow e^+ + e^-$ has been observed, corresponding to a dark matter particle of ∼450–1200 GeV [40].

There is a weak coupling of W^+W^- to $\gamma\gamma$ and the Higgs boson couples strongly to $t\bar{t}$, which has a weak coupling into two photons. Quark-antiquark pairs may transform into $\chi + \bar{\chi}$ via Z or H bosons.

As we have shown in reference [1] we may reach energy densities of 10^{12} GeV/fm^3 in the $n\gamma-m\gamma$ collider for 1 GeV γ beams and thus may study both phase transitions. The energy density for the quark-gluon-plasma $\epsilon_0 * (T/T_c)^4$ has typical values of $\epsilon_0 = 3$ GeV/fm^3 and $T_c = 170$ MeV. Extending this scaling law to our maximum reachable energy density of 10^{12} GeV/fm^3, it would correspond to a temperature of 170 GeV. Thus we will produce these phase transitions at lower temperatures but high densities. This is the most interesting situation, where we again may observe an enhanced stimulated production of BEC's of these bosons.

In the diagnostics we will search for particles with large transverse momentum from the decay of the exotic particles. Extremely high multiplicities of hadrons will occur, exceeding the capabilities of present high-energy physics detectors. So focusing on the exotic decays is reasonable.

8 Consequences for the ELI-facility

Many requirements for ELI can be deduced for the realization of such an $n\gamma-m\gamma$-collider. We ask for very intense single cycle pulses with very good contrast and very good pointing stability. It would be desirable to have a laser system with a high repetition rate (10 Hz) and an intensity of 10^{23} W/cm^2. The collider requires a special design, where the DLC foils can be changed with the same rate.

Compared to LHC, where one 7 TeV proton interacts with another 7 TeV proton, resulting in a local energy density of 10^4 GeV/fm^3, while this value in our case amounts to 10^{13} GeV/fm^3. Thus we have a 10^9 times larger energy density and 10^9 times more reaction products than the LHC. CERN shows that the granularity and cost of calorimeters or TCPs would rise very much if one would be interested in identifying all particles. So it seams advantageous to focus on more rare particles with large transverse momenta. Still a large detector system of at least 15 m^3 is required in a concrete cave with several meter thick walls.

9 Conclusions

We should focus in the beginning on a $n\gamma-m\gamma$-collider with lower photon energies like 10 keV, where the problems of reflectivity and diffraction limited focusing are reduced and not even the highest intensities or the best focusing are required to produce e^+e^--pairs. The new production scheme of the γ rays has the advantage that the same relativistic mirror is used for the production and the focusing. The larger interaction volume, due to the larger wave length, results in a colder e^+e^- plasma with a higher probability of Ps formation. Interesting multi-positronium physics can be studied and the annihilation of the Ps allows for a good diagnostics. For shorter wave length photons we reach higher energy densities with higher temperatures and the $e^+e^-\gamma$ plasma produces hadrons.

We acknowledge many useful discussions with J. Wambach, D. Rischke, S. Typel, M. Thoma and O. Biebel. Supported by Deutsche Forschungsgemeinschaft through the DFG-Cluster of Excellence Munich-Centre for Advanced Photonics (MAP) and Transregio TR18. The authors acknowledge the support by the European Commission under contract ELI pp 212105 in the framework of the program FP7 Infrastructures-2007-1.

References

1. D. Habs et al., Appl. Phys. B **93**, 349 (2008)
2. D. Kiefer et al., Eur. Phys. J. D **55**, 427 (2009)
3. L.D. Landau, E.M. Lifshitz, *Lehrbuch der theoretischen Physik* (Akademie, 1986 Berlin), Vol. IV
4. S.V. Bulanov et al., J. Exp. Theor. Phys. **102**, 9 (2006)
5. A. Sessler, Phys. Today **51**, 48 (1998)
6. V.G. Serbo, *Basics of a Photon Collider* (2005) arXiv:hep-ph/0510335v2
7. G. Baur et al., Phys. Rep. **364**, 359 (2002)
8. O. Klimo et al., Phys. Rev. ST Accel. Beams **11**, 031301 (2008)
9. V.V. Kulagin et al., Phys. Rev. Lett. **99**, 123801 (2007)
10. A. Einstein, Annalen der Physik **17**, 891 (1905)
11. A.S. Pirozhkov et al., Phys. Plasmas **14**, 123106 (2007)
12. A.V. Panchenko, T.Zh. Esirkepov, A.S. Pirozhkov, M. Kando, F.F. Kamenets, S.V. Bulanov, Phys. Rev. E **78**, 056402 (2008)
13. F.E. Low, Phys. Rev. **120**, 582 (1960)
14. Particle Data Group, Phys. Lett. B **667**, 363 (2008)
15. A. Ringwald, DESY 01-24 (2001) arXiv:hep-ph/0103185
16. A. Ringwald, Phys. Lett. B **510**, 107 (2001)
17. S.N. Bose, Z. Phys. **26**, 178 (1924)
18. A. Einstein, Physikalisch-mathematische Klasse (Berlin) **22**, 261 (1924); A. Einstein, Physikalisch-mathematische Klasse (Berlin) **22**, 3 (1925)
19. A.P. Mills, Nucl. Instrum. Meth. B **192**, 107 (2002)
20. V.V. Begun, M.I. Gorenstein, Phys. Rev. C **77**, 064903 (2008)
21. A. Griffin, D.W. Snoke, S. Stringari, *Bose-Einstein Condensation* (Cambridge University Press, 1995)
22. A.J. Leggett, *Quantum Liquids*, Oxford Graduate Texts (Oxford University Press, 2006)
23. V.S. Popov, J. Exp. Theor. Phys. Lett. **74**, 151 (2001)
24. M. Deutsch, Phys. Rev. **82**, 455 (1951)
25. S. Berko, H.N. Pendleton, Ann. Rev. Nucl. Part. Sci. **30**, 543 (1980)
26. J.A. Wheeler, Ann. NY Acad. Sci. **48**, 219 (1946)
27. A.P. Mills, Phys. Rev. Lett. **46**, 717 (1981)
28. K. Varga et al., Phys. Rev. Lett. **80**, 1876 (1998)
29. D.B. Cassidy, A.P. Mills, Nature **449**, 195 (2007)
30. D.M. Schrader, Phys. Rev. Lett. **92**, 043401 (2004)
31. Y.K. Ho, Phys. Rev. A **33**, 3584 (1986)
32. P.M. Platzmann, A.P. Mills, Phys. Rev. B **49**, 454 (1994)
33. T. Schäfer, *Quark Matter* (2003) arXiv:hep-ph/0304281v2
34. M. Buballa, Prog. Part. Nucl. Phys. **61**, 66 (2008)
35. J. Delorme, M. Erison, T.E.O. Ericson, Phys. Lett. B **291**, 379 (1992)
36. M. Thoma, Eur. Phys. J. D **55**, 271 (2009)
37. I. Kuznetsova, D. Habs, J. Rafelski, Phys. Rev. D **78**, 014027 (2008)

38. J. Meyer-ter-Vehn et al., Phys. Plasmas **8**, 1003 (2001)
39. P. Jacobs et al., Prog. Part. Nucl. Phys. **54**, 443 (2005)
40. D. Elsässer et al., Phys. Rev. Lett. **94**, 171302 (2005); J. Hall et al. (2008) arXiv:astro-ph/0811.3362v1
41. International Centre for Theoretical Physics, Trieste, Internal Report, IC/92/152, (1992)
42. A.M. Frolov, Phys. Rev. A **60**, 2834 (1999)
43. D.B. Kinghorn, R.D. Poshusta, Phys. Rev. A **47**, 3671 (1993)
44. S.H. Adhirai, Phys. Lett. A **294**, 308 (2002)
45. Ch. Berger, W. Wagner, Phys. Rep. **146**, 1 (1987)
46. C. Itzykson, J.-B. Zuber, *Quantum Field Theory* (Mc Graw-Hill International Book Company, 1980)
47. S.V. Bulanov et al., Phys. Rev. Lett. **91**, 085001 (2003)